The effect of subgrid-scale models on grid-scale/subgrid-scale energy transfers in large-eddy simulation of incompressible magnetohydrodynamic turbulence

M. Kessar, G. Balarac, and F. Plunian

Citation: Physics of Plasmas **23**, 102305 (2016); doi: 10.1063/1.4964782
View online: http://dx.doi.org/10.1063/1.4964782
View Table of Contents: http://scitation.aip.org/content/aip/journal/pop/23/10?ver=pdfcov
Published by the AIP Publishing

The effect of subgrid-scale models on grid-scale/subgrid-scale energy transfers in large-eddy simulation of incompressible magnetohydrodynamic turbulence

M. Kessar,[1,2] G. Balarac,[1] and F. Plunian[2]
[1]*University Grenoble Alpes, CNRS, LEGI, Grenoble, France*
[2]*University Grenoble Alpes, CNRS, ISTerre, Grenoble, France*

(Received 20 July 2016; accepted 27 September 2016; published online 18 October 2016)

In this work, the accuracy of various models used in large-eddy simulations (LES) of incompressible magnetohydrodynamic (MHD) turbulence is evaluated. Particular attention is devoted to the capabilities of models to reproduce the transfers between resolved grid- and subgrid-scales. The exact global balance of MHD turbulent flows is first evaluated from direct numerical simulation (DNS) database. This balance is controlled by the transfers between scales and between kinetic and magnetic energies. Two cases of forced homogeneous isotropic MHD turbulent flows are considered, with and without injecting large scale helicity. The strong helical case leads to domination of the magnetic energy due to an inverse cascade [A. Brandenburg, Astrophys. J. **550**(2), 824 (2001); N. E. Haugen *et al.*, Phys. Rev. E **70**(1), 016308 (2004)]. The energy transfers predicted by various models are then compared with the transfer extracted from DNS results. This allows to discriminate models classically used for LES of MHD turbulence. In the non-helical case, the Smagorinsky-like model [M. L. Theobald *et al.*, Phys. Plasmas **1**, 3016 (1994)] and a mixed model are able to perform stable LES, but the helical case is a more demanding test and all the models lead to unstable simulations. *Published by AIP Publishing.*
[http://dx.doi.org/10.1063/1.4964782]

I. INTRODUCTION

For many geophysical and astrophysical applications, magnetohydrodynamics (MHD) flows must be taken into consideration. For example, MHD is crucial to the study of solar activities, where understanding the formation of magnetic regions in the upper turbulent convective boundary layer of the Sun is particularly important for local helioseismology and helioseismic data analysis. Another example is related to the study of the Earth's large-scale magnetic field, which may be generated by turbulence in the Earth's core. However, in these applications, the Reynolds number leads to turbulent flows with a very wide range of motion and magnetic scales. This range is too large for direct numerical simulation (DNS), with an explicit description of all scales. However, with the development of computational power, it can be expected that realistic simulations can be performed by using large-eddy simulations (LES). The LES technique proposes to explicitly solve only the large scales of the MHD flow and to model the impact of the smallest scales on the large scales. Since the large scales are determined from the grid mesh, they are referred as "grid scales" (GS), whereas the small unresolved scales are referred as the "subgrid scales" (SGS). SGS models are then used to close the LES governing equations.

Several works have been devoted to the development of SGS models for hydrodynamic[4–6] and magnetohydrodynamic[3,7,8] flows. Due to the scale separation implied by LES, an accurate approach is to develop the models in Fourier space.[5,7] However, this kind of model can only be used for simulations performed in this space, through spectral solvers. Therefore, this approach cannot easily deal with the complex geometry, and LES models expressed in physical space have been proposed,[3,9–11] as they are easier to implement in classic finite volume or finite difference solvers. In this work, only SGS models expressed in physical space are considered.

The evaluation of SGS model performance is mainly performed by comparison with DNS, with experiment or with observation. Thus, for LES of MHD turbulence, various models have been evaluated by comparison with observations of the Sun[12] or observations of the Earth's magnetic field.[13] DNS comparisons have also been performed in incompressible[8,14,15] and compressible[16] decaying and forced turbulence, or for geodynamo configurations.[11,17] In this work, DNS with higher resolutions is used to evaluate the SGS models with larger hydrodynamic and magnetic Reynolds numbers, in comparison with previous studies.[8,15,16] Moreover, forced homogeneous isotropic turbulence is considered with two different forcing schemes without and with helicity injection. Both cases lead to the production of magnetic energy due to the dynamo effect, but the second forcing scheme leads to the presence of an inverse cascade of magnetic energy. This flow configuration has never been used for the evaluation of models used in LES.

The evaluation of SGS models is mainly focused on their capabilities to reproduce GS/SGS energy transfers. After the DNS database is presented (Section II), exact equations of the GS/SGS kinetic and magnetic energies will be derived (Section III). This allows the definition of the global energy balance of the flow and the identification of the GS/SGS transfer terms for both kinetic and magnetic energies. From the DNS database, it is shown that the energy balance and the GS/SGS transfer terms are strongly dependent on the flow configurations. Finally, several sets of models proposed for LES of MHD turbulent flows will be evaluated by comparison with DNS database results (Section IV).

II. DNS DATABASE

A. Governing equations and numerical tools

To analyze the energy transfers and to evaluate LES modeling strategies, a DNS database is used. The simulations are performed by solving the set of equations governing the MHD turbulent flow on the entire range of scales. This set of equations is composed by the transport equations of the flow velocity, $\vec{u}$, and the magnetic field, $\vec{b}$, expressed for convenience in Alfven-speed units. In the incompressible case, this set of equations writes, using Einstein's notation,

$$\partial_t u_i + u_j \partial_j u_i = -\partial_i \Pi + b_j \partial_j b_i + \nu \partial_{jj} u_i + f_i, \quad (1)$$

$$\partial_t b_i + u_j \partial_j b_i = b_j \partial_j u_i + \eta \partial_{jj} b_i, \quad \text{and} \quad (2)$$

$$\partial_i u_i = \partial_i b_i = 0. \quad (3)$$

In these equations, Π is the total pressure (including the magnetic pressure), $\Pi = p + b_i b_i/2$ (with p the thermodynamic pressure), and $\vec{f}$ is an external forcing. The fluid density is assumed to be constant, equal to unity. The properties of the flow are defined by the molecular viscosity, ν, and the magnetic diffusivity, η. In this work, the set of Equations (1)–(3) is solved in a computational domain of length 2π with periodic boundary conditions in three directions, by using a pseudo-spectral code with the second-order explicit Runge-Kutta time advancement for both transport equations. The viscous and diffusive terms are treated exactly, and a classic 2/3 rule is used for de-aliasing the non-linear terms.[18] This code has been validated in various turbulent configurations, including turbulent mixing and MHD turbulent flows.[19–21]

B. Flow configuration

In this study, the DNS database consists of forced homogeneous isotropic turbulence cases. In these cases, the magnetic field and the velocity field are first initialized as white noise, with an initial magnetic energy much smaller than the kinetic energy. The kinetic energy is then maintained by using a forcing term in Eq. (1). The magnetic energy grows due to dynamo effect,[1,2] without external forcing in the magnetic field in Eq. (2). This leads to a statistical stationary state, and the analyses are performed when the flow is statistically steady.

Two simulations are performed to reproduce different MHD turbulent flow behaviors. The simulations differ by the forcing scheme used to inject kinetic energy within the flow. The forcing scheme proposed by Alvelius[22] is used first. This forcing allows the generation of homogeneous isotropic turbulence, without any injection of helicity within the flow. The second type of forcing is a modification of the first one, allowing the introduction of a large part of kinetic helicity in the flow. In this work, the first forcing scheme is referred to as non-helical forcing, whereas the second forcing scheme is referred to as helical forcing. Both forcing schemes are local in spectral space and are centered around the wave number, $k_f = \pi/l$, with l, the forcing scale: k_f is roughly equal to 2 and 4 for the non-helical and helical cases, respectively. Both simulations are performed for a magnetic Prandtl number (the viscosity to magnetic diffusivity ratio, $P_m = \nu/\eta$) equal to one, and both simulations are performed by using 512^3 grid points. This allows to perform simulations with a Reynolds number based on the Taylor micro-scales, R_λ, equal to 75 and 55 for the non-helical and helical cases, respectively. The choice P_m equals to unity is probably the best one in terms of optimization of the computer resources for a dynamo simulation. Indeed, for a given value of R_λ, if P_m is too small then the dynamo disappears, whereas if P_m is larger than unity, then the magnetic spectra extend to smaller scales needing more computer resources.

Figure 1 shows the time evolution of the mean kinetic energy, $e_k = 1/2\langle u_i u_i \rangle$, and of the mean magnetic energy, $e_m = 1/2\langle b_i b_i \rangle$, with the brackets indicating a volume averaging. As expected, in both cases, a first stage consists of a growth of the magnetic energy and a slight decrease in the kinetic energy, until a saturated regime leads to a statistically stationary state in case (a) and a magnetic energy still slightly increasing in case (b). The growth of the magnetic energy and the decrease in the kinetic energy are due to the dynamo effect, which implies a transfer from the (forced) kinetic energy to the (unforced) magnetic energy. Both cases differ then at the saturated regime. Indeed, for the non-helical forcing case, a large part of the total energy is still composed by the kinetic energy, whereas for the helical forcing case, the magnetic energy becomes higher than the

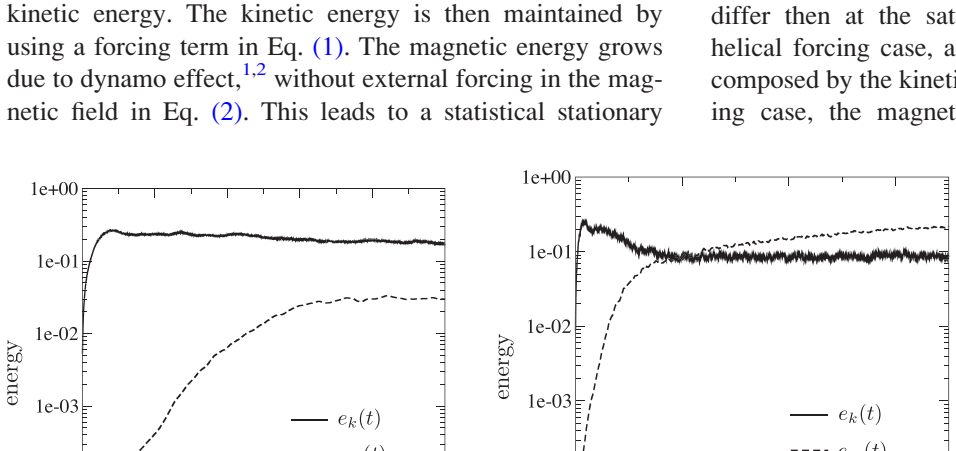

FIG. 1. Time evolution of mean kinetic energy, $e_k(t)$, and mean magnetic energy, $e_m(t)$, for both non-helical forcing (a) and helical forcing (b) cases.

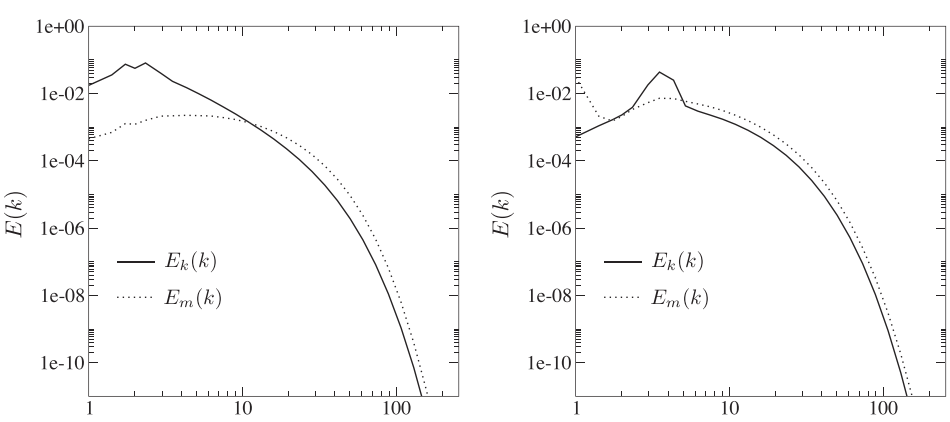

FIG. 2. Kinetic, $E_k(k)$, and magnetic, $E_m(k)$, energy spectra for both non-helical forcing (a) and helical forcing (b) cases.

kinetic energy. In Figure 2, the kinetic and magnetic energy spectra are plotted in the saturated regime. In both cases, a quasi equipartition between kinetic and magnetic energies occurs at the small scales (large wave numbers). However, differences appear at large scales. In the helical case, the magnetic energy spectrum has significant growth at smallest wave numbers, due to an inverse cascade.[1] Conversely, the non-helical case is dominated by the kinetic energy at the largest scales, without inverse cascade.[2] These conclusions are consistent with the instantaneous visualization of the magnetic field at the saturated regime shown in Figure 3. In the helical case, the generation of the magnetic field at large scales leads to a non-isotropic magnetic field with a preferential direction, whereas in the non-helical case, the magnetic field is isotropic.

III. LES FORMALISM AND GS/SGS ENERGY TRANSFERS

A. LES governing equations

As already stated, the goal of this work is to better understand the performance of previously proposed SGS models to perform LES of MHD turbulent flow. The LES technique proposes to explicitly solve the flow only for scales larger than a given scale Δ and to model the interactions between these large resolved scales (GS) and the small scales (SGS). This scale separation is performed by a filtering operation

$$\bar{f}(\vec{x}) = \int f(\vec{y}) G_\Delta(\vec{x}-\vec{y}) d\vec{y}, \tag{4}$$

where $\bar{f}$ is the filtered quantity corresponding to a flow field f, and G_Δ is the filter kernel associated with the filter size Δ. These equations, which have to be solved in LES, are obtained by applying the filtering operation at Eqs. (1)–(3), leading to the LES governing equations

$$\partial_t \bar{u}_i + \bar{u}_j \partial_j \bar{u}_i = -\partial_i \bar{\Pi} + \bar{b}_j \partial_j \bar{b}_i + \nu \partial_{jj} \bar{u}_i - \partial_j (\tau^u_{ij} - \tau^b_{ij}) + \bar{f}_i, \tag{5}$$

$$\partial_t \bar{b}_i + \bar{u}_j \partial_j \bar{b}_i = \bar{b}_j \partial_j \bar{u}_i + \eta \partial_{jj} \bar{b}_i - \partial_j \tau^{ub}_{ij}, \quad \text{and} \tag{6}$$

$$\partial_t \bar{u}_i = \partial_i b_i = 0, \tag{7}$$

where $\bar{u}_i$ and $\bar{b}_i$ are, respectively, the component of the filtered velocity and magnetic fields in the ith direction and $\bar{\Pi}$ is the filtered total pressure, $\bar{\Pi} = \bar{p} + \overline{b_i b_i}/2$. Due to the non-linear terms, the filtering operation leads to the following SGS tensors:

$$\tau^u_{ij} = \overline{u_i u_j} - \bar{u}_i \bar{u}_j, \tag{8}$$

$$\tau^b_{ij} = \overline{b_i b_j} - \bar{b}_i \bar{b}_j, \quad \text{and} \tag{9}$$

$$\tau^{ub}_{ij} = \overline{b_i u_j} - \bar{b}_i \bar{u}_j - (\overline{u_i b_j} - \bar{u}_i \bar{b}_j). \tag{10}$$

The first tensor, τ^u_{ij}, is related to the advection term, whereas the second tensor, τ^b_{ij}, is related to the Lorentz force term in the Navier-Stokes equation. These tensors are often referred to as the SGS Reynolds and Maxwell stress tensors, respectively. The last tensor, τ^{ub}_{ij}, derives from the filtering of the induction term in the magnetic field transport equation. When LES are performed, these SGS tensors are not explicitly known. They

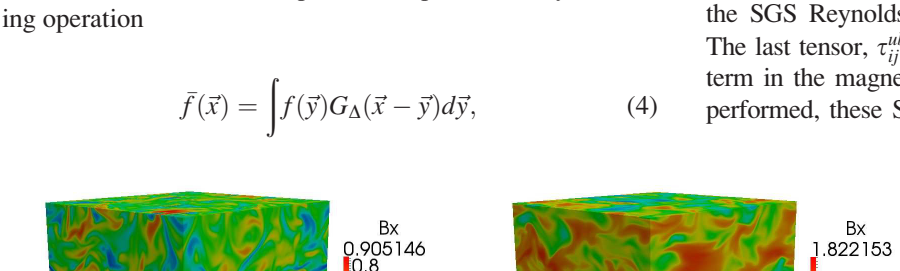

FIG. 3. Visualization of the x component of the magnetic field for the non-helical (a) and helical (b) cases.

have to be estimated by SGS models, assuming relationships with resolved quantities. Various works have addressed the modeling of these three SGS tensors for LES of MHD flows.[8,14,17] The goal of this work is to better analyze the GS/SGS energy transfers and to better measure the capabilities of SGS models to reproduce these transfers. Note that in the case of hydrodynamic (no MHD) turbulence, only the first tensor, τ^u_{ij}, has to be modeled to close the LES equations.

B. GS and SGS energy transport equations

A first step to better understand the interaction between grid scales (GS) and subgrid scales (SGS) consists of writing out the transport equations for the GS and SGS energies, as previously done in hydrodynamic turbulence.[23] In MHD turbulent flows, both kinetic and magnetic energies must be considered. The exact exchanges between GS/SGS energies and between kinetic and magnetic energies will appear. Thus, the transport equations for the GS kinetic energy, $E_{\bar{u}} = 1/2\bar{u}_i\bar{u}_i$, for the SGS kinetic energy, $E_{\tilde{u}} = 1/2\tau^u_{ii}$, for the GS magnetic energy, $E_{\bar{b}} = 1/2\bar{b}_i\bar{b}_i$, and for the SGS magnetic energy, $E_{\tilde{b}} = 1/2\tau^b_{ii}$, are given by

$$\partial_t E_{\bar{u}} = +T^{\bar{u}}_{\bar{u}} + T^{\bar{u}}_{\tilde{b}} - \epsilon_{\bar{u}} + D_{\bar{u}} + F_{\bar{u}}, \tag{11}$$

$$\partial_t E_{\tilde{u}} = -T^{\tilde{u}}_{\tilde{u}} + T^{\tilde{u}}_{\tilde{b}} - \epsilon_{\tilde{u}} + D_{\tilde{u}} + F_{\tilde{u}}, \tag{12}$$

$$\partial_t E_{\bar{b}} = +T^{\bar{b}}_{\bar{b}} - T^{\bar{u}}_{\bar{b}} - \epsilon_{\bar{b}} + D_{\bar{b}}, \tag{13}$$

$$\partial_t E_{\tilde{b}} = -T^{\tilde{b}}_{\tilde{b}} - T^{\tilde{u}}_{\tilde{b}} - \epsilon_{\tilde{b}} + D_{\tilde{b}}. \tag{14}$$

The left-hand-side of these equations represents the time variation of energy. For each equation, the energy time variation is in equilibrium with various terms representing various effects: external energy injection (noted F), diffusion (noted D), dissipation (noted ϵ), and transfer (noted T). The external energy injection is the kinetic energy fluxes injected by the external forcing. $F_{\bar{u}} = 1/2\bar{f}_i\bar{u}_i$ and $F_{\tilde{u}} = 1/2(\overline{f_iu_i} - \bar{f}_i\bar{u}_i)$ are the external energy injection for the GS and SGS kinetic energies, respectively. The diffusion effects are redistributions of energy. The diffusions terms are, respectively,

$$\begin{aligned}
D_{\bar{u}} &= \partial_j(-\bar{u}_jE_{\bar{u}} - \bar{\Pi}\bar{u}_i + \nu\partial_jE_{\bar{u}} - \bar{u}_i\tau^u_{ij} + \bar{u}_i\tau^b_{ij}),\\
D_{\tilde{u}} &= \partial_j\Big(-\bar{u}_jE_{\tilde{u}} - (\overline{u_i\Pi} - \bar{u}_i\bar{\Pi}) + \nu\partial_jE_{\tilde{u}} + \bar{u}_i\tau^u_{ij}\\
&\quad - \bar{u}_i\tau^b_{ij} - \frac{1}{2}(\overline{u_iu_iu_j} - \overline{u_iu_i}\bar{u}_j)\Big),\\
D_{\bar{b}} &= \partial_j(-\bar{u}_jE_{\bar{b}} + \bar{b}_j\bar{b}_i\bar{u}_i + \eta\partial_jE_{\bar{b}} - \bar{b}_i\tau^{ub}_{ij}),
\end{aligned}$$

and

$$D_{\tilde{b}} = \partial_j\Big(-\bar{u}_jE_{\tilde{b}} + (\overline{b_jb_iu_i} - \bar{b}_j\bar{b}_i\bar{u}_i) + \eta\partial_jE_{\tilde{b}} + \bar{b}_i\tau^{ub}_{ij} - \frac{1}{2}(\overline{b_ib_iu_j} - \overline{b_ib_i}\bar{u}_j)\Big).$$

Note that these terms can be grouped in a divergence form, meaning that the volume averaging of all these diffusion terms will be equal to zero in our flow configuration (with periodic boundary conditions in three directions), showing that these terms do not participate to the global energy balance. Diffusion effects consist only in a spatial re-distribution of energy. Conversely, the dissipation effect is an energy loss. Dissipation effects correspond to the transformation of energy in heat due to the molecular viscosity for the kinetic energy and the molecular magnetic diffusivity for the magnetic energy. In Eqs. (11)–(14), the dissipations terms can be written as

$$\begin{aligned}
\epsilon_{\bar{u}} &= \nu(\partial_j\bar{u}_i)^2,\\
\epsilon_{\tilde{u}} &= \nu\Big(\overline{(\partial_ju_i)^2} - (\partial_j\bar{u}_i)^2\Big),\\
\epsilon_{\tilde{b}} &= \eta(\partial_j\bar{b}_i)^2,
\end{aligned}$$

and

$$\epsilon_{\tilde{b}} = \eta\Big(\overline{(\partial_jb_i)^2} - (\partial_j\bar{b}_i)^2\Big).$$

The last effects are the energy transfer effects. There are two types of energy transfers. The first type is the transfer between kinetic and magnetic energies. Then, these transfer terms appear with opposite sign in the transport equations of GS kinetic and magnetic energies

$$T^{\bar{u}}_{\bar{b}} = \bar{u}_i\partial_j(\bar{b}_j\bar{b}_i),$$

and in the transport equation of the SGS kinetic and magnetic energies

$$T^{\tilde{u}}_{\tilde{b}} = \overline{u_i\partial_j(b_jb_i)} - \bar{u}_i\partial_j(\bar{b}_j\bar{b}_i).$$

It is this kind of transfers which leads to dynamo phenomenon. Finally, the second type of transfers is between grid-scale (GS) and subgrid-scale (SGS) energy. The transfer of GS and SGS magnetic energies is due to the induction term

$$T^{\bar{b}}_{\tilde{b}} = \bar{J}_{ij}\tau^{ub}_{ij},$$

with $\bar{J}_{ij} = 1/2(\partial_j\bar{b}_i - \partial_i\bar{b}_j)$, the GS magnetic rotation tensor. This term appears then with the opposite sign in the transport equations of GS and SGS magnetic energies. The transfer term of GS and SGS kinetic energies appears with the opposite sign in the transport equations of GS and SGS kinetic energies, and it is written as

$$T^{\bar{u}}_{\tilde{u}} = \bar{S}^u_{ij}\tau^u_{ij} - \bar{S}^u_{ij}\tau^b_{ij} = T_{A^{\bar{u}}_{\tilde{u}}} + T_{L^{\bar{u}}_{\tilde{u}}},$$

with $\bar{S}^u_{ij} = 1/2(\partial_j\bar{u}_i + \partial_i\bar{u}_j)$, the GS deformation tensor. This shows that the transfer of kinetic energy between grid and subgrid scales is due to both effects: the advection term, $T_{A^{\bar{u}}_{\tilde{u}}} = \bar{S}^u_{ij}\tau^u_{ij}$, as in hydrodynamic (no MHD) turbulence, but also the Lorentz force term, $T_{L^{\bar{u}}_{\tilde{u}}} = -\bar{S}^u_{ij}\tau^b_{ij}$, specific to MHD turbulence. These GS/SGS transfer terms can act as either a "sink" term for the GS energy, meaning the transfer from GS to SGS (forward scatter), or as a source term, meaning an inverse transfer (backward scatter).

C. GS/SGS energy transfers from filtered DNS

Based on the transport equations of GS and SGS energies, Eqs. (11)–(14), the mean energy balances can be

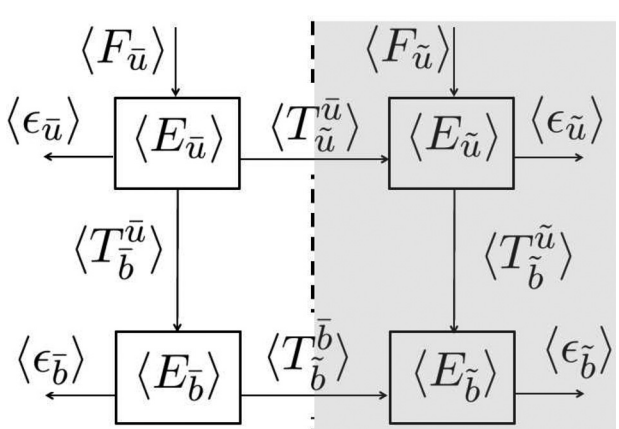

FIG. 4. Mean energy balance in the context of LES of MHD turbulent flows. Due to the scale separation at the filter size Δ, energy is split in GS and SGS part, noted $E_{\bar{u}}$ and $E_{\tilde{u}}$ for the kinetic energy, and noted $E_{\bar{b}}$ and $E_{\tilde{b}}$ for the magnetic energy, respectively. The SGS part (in grey on the scheme) is the part which is not explicitly resolved in LES.

studied. The mean balance is obtained by a volume averaging, noted with brackets, $\langle . \rangle$, of the energy transport equations. As already explained, due to the averaging operator, all the diffusion terms (written as divergence terms) will be zero. Moreover, the study is performed in a saturated regime; the flow is then statistically stationary, and the averaged time-variation terms are negligible. Only a few terms control the energy balance. The global energy balance can be written as

$$+\langle T^{\bar{u}}_{\tilde{u}} \rangle + \langle T^{\bar{u}}_{\bar{b}} \rangle - \langle \epsilon_{\bar{u}} \rangle + \langle F_{\bar{u}} \rangle = 0, \tag{15}$$

$$-\langle T^{\bar{u}}_{\tilde{u}} \rangle + \langle T^{\tilde{u}}_{\tilde{b}} \rangle - \langle \epsilon_{\tilde{u}} \rangle + \langle F_{\tilde{u}} \rangle = 0, \tag{16}$$

$$+\langle T^{\bar{b}}_{\tilde{b}} \rangle - \langle T^{\bar{u}}_{\bar{b}} \rangle - \langle \epsilon_{\bar{b}} \rangle = 0, \tag{17}$$

$$-\langle T^{\bar{b}}_{\tilde{b}} \rangle - \langle T^{\tilde{u}}_{\tilde{b}} \rangle - \langle \epsilon_{\tilde{b}} \rangle = 0. \tag{18}$$

The global energy balance can then be summarized by the scheme shown in Figure 4. The balance is given by energy injection, molecular dissipation of each energy, and transfers between energies. In LES, only GS energies are explicitly solved, and the SGS stress tensors (τ^u_{ij}, τ^b_{ij}, and τ^{ub}_{ij}) have to be modeled. Because the GS/SGS transfer terms, $T^{\bar{u}}_{\tilde{u}}$ and $T^{\bar{b}}_{\tilde{b}}$, involve the SGS stress tensors, an inaccurate modeling of these tensors will yield an incorrect representation of the energy balance. To better understand the transfers occurring in MHD flows, the energy balances are computed from the DNS database. Note that all the results are shown as a function of the filter size to vary the separation between grid-scales (GS) and subgrid-scales (SGS) quantities.

Figure 5 shows first the SGS kinetic energy balance for both cases of the DNS database. The SGS kinetic energy balance is shown as a function of the filter width. For a large part, the filter width is smaller than the forcing scale, and then, the SGS kinetic energy injection $\langle F_{\tilde{u}} \rangle$ is zero. In this case, the balance is between the molecular dissipation $\langle \epsilon_{\tilde{u}} \rangle$, the SGS transfer between kinetic and magnetic energies, $\langle T^{\tilde{u}}_{\tilde{b}} \rangle$, and the GS/SGS transfer terms, $\langle T_{A^{\bar{u}}_{\tilde{u}}} \rangle$ and $\langle T_{L^{\bar{u}}_{\tilde{u}}} \rangle$. Note that only the molecular dissipation is a net loss of energy. In this figure, negative value means that the term acts as a "sink" term with a loss of the considered energy (here, the SGS kinetic energy), whereas a positive value means that the term acts as a "source" term with a gain of energy. For both cases, for small filter sizes, the SGS part of the energy is negligible because no transfer occurs from GS to SGS. When the filter size increases, the transferred part of the GS kinetic energy towards the SGS kinetic energy, terms $\langle T_{A^{\bar{u}}_{\tilde{u}}} \rangle$ and $\langle T_{L^{\bar{u}}_{\tilde{u}}} \rangle$, increases. The positive value of $-\langle T_{A^{\bar{u}}_{\tilde{u}}} \rangle$ and $-\langle T_{L^{\bar{u}}_{\tilde{u}}} \rangle$ corresponds to a global direct transfer from GS to SGS (forward scatter). Then, the SGS kinetic energy is not negligible. The balance is between the "source" term due to the GS/SGS transfers and the "sink" term due to the molecular dissipation and the transfer $\langle T^{\tilde{u}}_{\tilde{b}} \rangle$. Indeed, the term $\langle T^{\tilde{u}}_{\tilde{b}} \rangle$ is negative, showing that the transfer is mainly from the SGS kinetic to SGS magnetic energies. Finally, if the filter width is smaller than the forcing scale (i.e., where the SGS kinetic energy injection is zero), the global equilibrium for the SGS kinetic energy is

$$\langle T_{A^{\bar{u}}_{\tilde{u}}} \rangle + \langle T_{L^{\bar{u}}_{\tilde{u}}} \rangle = \langle T^{\tilde{u}}_{\tilde{b}} \rangle - \langle \epsilon_{\tilde{u}} \rangle. \tag{19}$$

Even if the previous observations are true for both cases, some differences can be evoked, in particular, for terms $\langle T_{A^{\bar{u}}_{\tilde{u}}} \rangle$ and $\langle T_{L^{\bar{u}}_{\tilde{u}}} \rangle$, which are terms that depend on τ^u_{ij} and τ^b_{ij}, the SGS tensors modeled to perform LES. It is interesting to note that

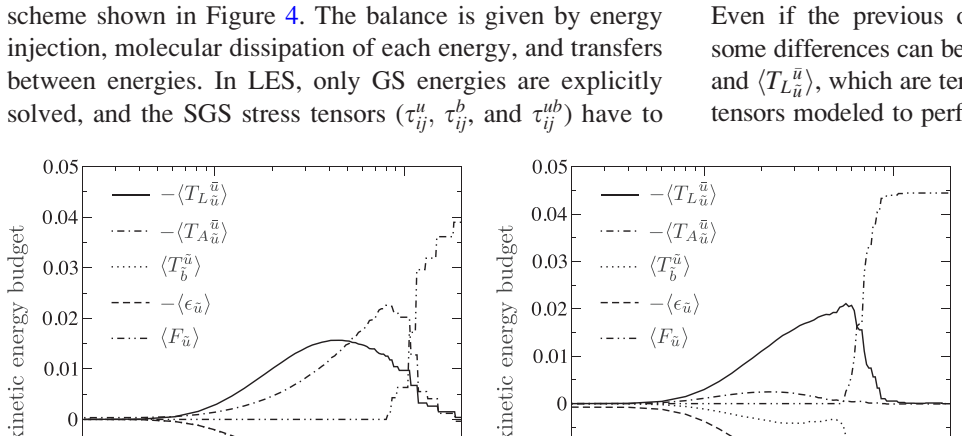

FIG. 5. Averaged budget of the SGS kinetic energy given by Eq. (16) with $\langle T^{\bar{u}}_{\tilde{u}} \rangle = \langle T_{L^{\bar{u}}_{\tilde{u}}} \rangle + \langle T_{A^{\bar{u}}_{\tilde{u}}} \rangle$, for the non-helical (a) and helical (b) cases as a function of $\Delta/\Delta x$, with Δ the filter size and Δx the DNS grid resolution.

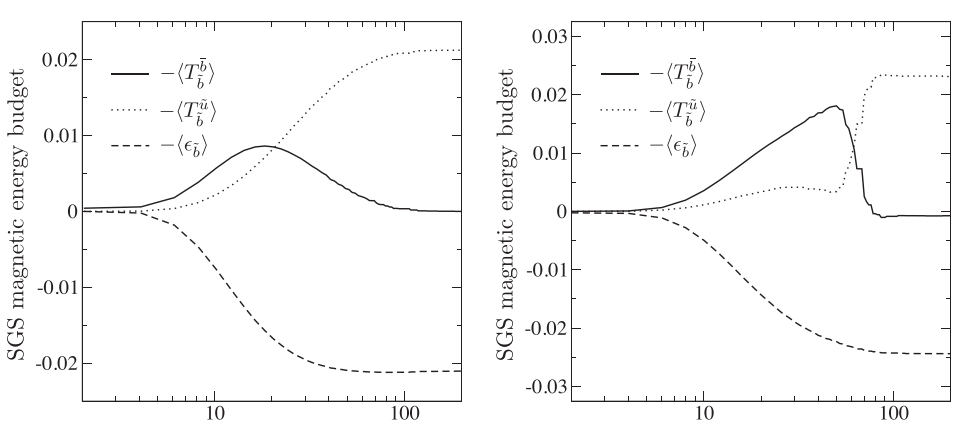

FIG. 6. Averaged budget of the SGS magnetic energy given by Eq. (18), for the non-helical (a) and helical (b) cases as function of $\Delta/\Delta x$.

the transfer due to the advection term $\langle T_{A^{\bar{u}}_{\tilde{u}}}\rangle$ and the transfer due to the Lorentz force term $\langle T_{L^{\bar{u}}_{\tilde{u}}}\rangle$ have similar amplitude in the non-helical case, whereas the GS/SGS transfers are mainly dominated by the Lorentz force in the helical case. For modeling purposes, this leads to a need for an appropriate set of models that are able to reproduce the relative amplitude of both advection and Lorentz force terms. Finally, a last remark can be done by a comparison with the hydrodynamic (without magnetic field) case. Indeed, in this case, only the transfer due to the advection exists as a "source" term and only the molecular dissipation act as a "sink" term. The global equilibrium is then only given by $\langle T_{A^{\bar{u}}_{\tilde{u}}}\rangle = -\langle \epsilon_{\tilde{u}}\rangle$. This assumption is the starting point of various SGS model for hydrodynamic LES. But in MHD LES, such simple assumption cannot be accurate. Indeed, results clearly show that the global equilibrium (19) cannot be split in more simple equilibrium as $\langle T_{A^{\bar{u}}_{\tilde{u}}}\rangle = -\langle \epsilon_{\tilde{u}}\rangle$, for example.

Figure 6 shows the mean SGS magnetic energy balance for both cases. The SGS magnetic energy is maintained by both transfer from the SGS kinetic energy (term $\langle T^{\tilde{u}}_{\tilde{b}}\rangle$) and the GS/SGS transfer of magnetic energy (term $\langle T^{\bar{b}}_{\tilde{b}}\rangle$). Then, also for magnetic energy, the GS/SGS transfer is positive, corresponding to a direct cascade of magnetic energy from large to small scales. Note that, in the helical case, a change from positive to negative in the GS/SGS transfer term appears for scales larger than the forcing scale ($\Delta/\Delta x > 70$) due to the inverse cascade existing at larger scale than the forcing scale.[24] Nevertheless, these scales will be in the range of the large resolved scales in LES context. Thus, even in this case, the SGS models need to reproduce mainly direct transfers of magnetic energy, for both helical and non-helical flows. Note that the modeling of inverse transfers (from SGS to GS) can be a delicate task, because this implies the injection of energy at the resolved scales, which can lead to numerical instabilities. The two transfer terms act as "source" term, and only the molecular dissipation (term $\langle \epsilon_{\tilde{b}}\rangle$) acts as "sink" term. The global equilibrium for the SGS magnetic energy can then be written as

$$\langle T^{\tilde{u}}_{\tilde{b}}\rangle + \langle T^{\bar{b}}_{\tilde{b}}\rangle = -\langle \epsilon_{\tilde{b}}\rangle. \tag{20}$$

Note that also in this case, the global equilibrium is more complex than the classic assumption "*production equal dissipation*," because two distinct phenomena act as production term. Moreover, the equilibria (19) and (20) are coupled (and at the GS level also). This means that if one of these equilibria is modified by the modeling of the GS/SGS transfers, all the other equilibria can be strongly modified. The LES modeling for the MHD flow is particularly challenging for this reason.

Deeper analyses of the GS/SGS transfers can be performed through the probability density function (PDF). Figures 7 and 8 show the PDF of terms $-T_{A^{\bar{u}}_{\tilde{u}}}$, $-T_{L^{\bar{u}}_{\tilde{u}}}$, and $-T^{\bar{b}}_{\tilde{b}}$ for $\Delta/\Delta x = 8$, for both cases. Even if the fluxes are mainly from the GS to the SGS as seen with the average value, the local inverse transfers (backscatter) exist, as shown by the negative tail of the PDF. Both tails (negative for the backward scatter and positive for the forward scatter) are large, meaning that GS/SGS transfers are very intermittent phenomena, with very strong fluctuations. For the non-helical case, the GS/SGS transfers of kinetic energy shown by the PDF are similar for $-T_{A^{\bar{u}}_{\tilde{u}}}$ and $-T_{L^{\bar{u}}_{\tilde{u}}}$. Conversely, in the helical case, the Lorentz force term dominates the advection term for both forward and backward scatters. For the GS/SGS magnetic energy transfer, Figures 7 and 8 show that in the helical case the positive tail decreases more slowly than in the non-helical case, whereas the negative tails remain similar in both cases. This means that the fluctuations of the magnetic GS/SGS transfers are much stronger in the presence of helicity, i.e., in the presence of a large-scale magnetic field.

IV. EFFECT OF SGS MODELS

The DNS database is now used to better understand the capabilities of various SGS models to accurately predict the GS/SGS transfers occurring in LES of MHD turbulent flows. The performance of the SGS models is measured based on both *a priori* and *a posteriori* tests. First, *a priori* tests emulate LES quantities by filtering DNS quantities and directly compare the GS/SGS transfers predicted by models with exact transfers. In this work, a spectral cut-off is used as the LES filter. *A posteriori* tests perform LES computations and compare filtered DNS and LES results.

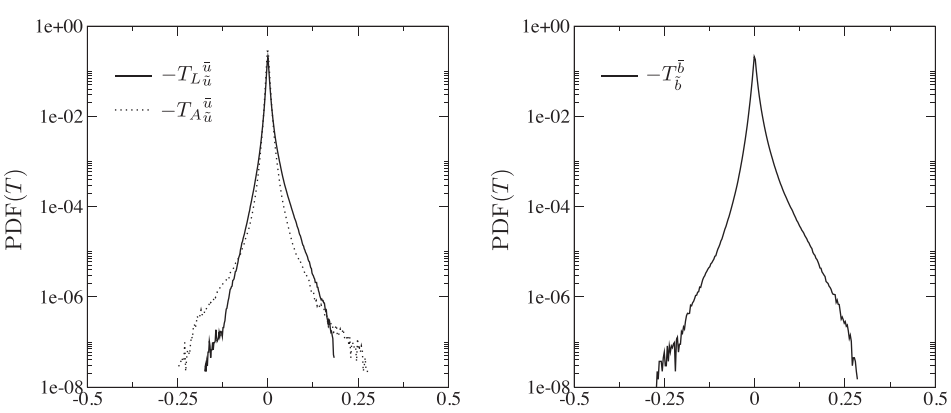

FIG. 7. Probability density function (PDF) of GS/SGS transfers for kinetic (a) and magnetic (b) energies at $\Delta/\Delta x = 8$, for the non-helical case.

A. Models definition

1. Smagorinsky-like model (Smag)

This model is based on the definition of eddy diffusivity and viscosity, to model the part of the GS energy transferred to the SGS energy by analogy with the molecular dissipation phenomenon. A classic definition of the eddy viscosity model in hydrodynamic flow was first introduced by Smagorinsky.[4] The MHD extension of this model was then proposed by Theobald *et al.*,[3] leading to the following set of expressions for the modeled closure terms:

$$\tau_{ij}^u - \tau_{ij}^b = C_\nu \Delta^2 |\bar{S}^u| \bar{S}_{ij}^u \quad \text{and} \tag{21}$$

$$\tau_{ij}^{ub} = C_\lambda \Delta^2 |\vec{\bar{j}}| \overline{J_{ij}}, \tag{22}$$

with $|\bar{S}^u| = (2\bar{S}_{ij}^u \bar{S}_{ij}^u)^{1/2}$, $\vec{j} = \vec{\nabla} \times \vec{b}$ the electric current density, and $|\vec{\bar{j}}| = (\vec{\bar{j}}.\vec{\bar{j}})^{1/2}$. C_ν and C_λ are coefficients to be determined. Based on a self-similarity assumption between the filter size and a larger scale, a numerical procedure can be proposed to compute the coefficients dynamically during the simulations.[25,26] This dynamic procedure has been applied for the MHD flow by Agullo *et al.*[14] Note that in the modeling of $\tau_{ij}^u - \tau_{ij}^b$, only quantities based on the velocity field are involved. This can appear as a weakness of the model for MHD turbulent flows where the magnetic energy dominates. This issue could be partially compensated by the dynamic procedure, since the magnetic field is taken into account in the computation of the coefficients. In this work, the Smagorinsky-like (Smag) model is evaluated using the dynamic procedure for C_ν and C_λ.

2. Cross-helicity model (Cross)

The cross-helicity (Cross) model was introduced by Müller and Carati,[8] and it is also based on eddy diffusivity and viscosity assumptions. The eddy viscosity and diffusivity are defined with quantities based on cross-helicity. Since the local dissipation of cross-helicity can be written as the sum of $\epsilon^{C_v} \sim |\bar{S}^u : \bar{S}^b|^{\frac{1}{2}}$ and $\epsilon^{C_b} \sim |\bar{j}_k.\bar{\omega}_k|^{1/2}$, the expressions of the model were given as follows:

$$\tau_{ij}^u - \tau_{ij}^b = -C_\nu \Delta^2 |\bar{S}^u : \bar{S}^b|^{1/2} \bar{S}_{ij}^u, \tag{23}$$

$$\tau_{ij}^{ub} = -C_\lambda \Delta^2 \mathrm{sgn}(\bar{j}_k \bar{\omega}_k) |\bar{j}_k \bar{\omega}_k|^{1/2} \bar{J}_{ij} \tag{24}$$

with $\bar{S}_{ij}^b$ being the magnetic strain rate tensor and $\vec{\omega} = \vec{\nabla} \times \vec{u}$ is the vorticity. Note that the term $\mathrm{sgn}(\bar{j}_k \bar{\omega}_k)$ was added in the model of τ_{ij}^{ub} in order to reproduce backward transfers of both magnetic helicity and magnetic energy.

3. Gradient model (Grad)

The gradient model was originally introduced by Leonard[9] for hydrodynamic turbulence. Thereafter, this model was applied to MHD flows by Müller and Carati[8] and was also used for geodynamo studies.[11,13,27] This model is a

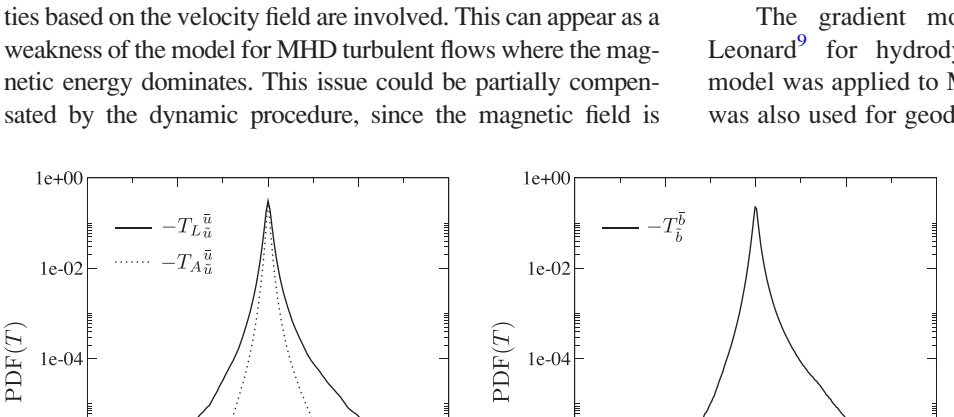

FIG. 8. Probability density function (PDF) of GS/SGS transfers for kinetic (a) and magnetic (b) energies at $\Delta/\Delta x = 8$, for the helical case.

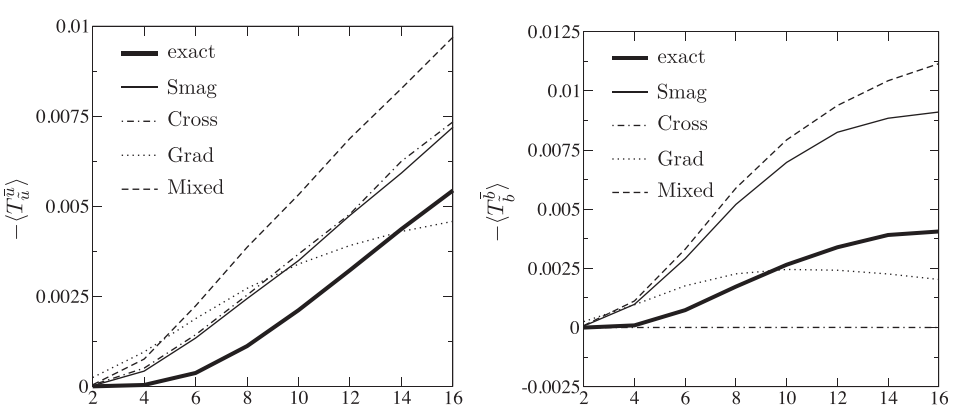

FIG. 9. Averaged GS/SGS transfers predicted by models as a function of the filter size, for both kinetic (left) and magnetic (right) energies, in the non-helical case. The exact transfers are also shown for comparison.

structural model based on the Taylor series expansion of the filtering operation. Applying the Taylor series expansion to the SGS tensors and keeping only the first terms, the gradient (Grad) model can be written as

$$\tau_{ij}^{u} = \frac{\Delta^2}{12}\frac{\partial \bar{u}_i}{\partial_k}\frac{\partial \bar{u}_j}{\partial_k}, \tag{25}$$

$$\tau_{ij}^{b} = \frac{\Delta^2}{12}\frac{\partial \bar{b}_i}{\partial_k}\frac{\partial \bar{b}_j}{\partial_k}, \tag{26}$$

$$\tau_{ij}^{ub} = \frac{\Delta^2}{12}\left(\frac{\partial \bar{b}_i}{\partial_k}\frac{\partial \bar{u}_j}{\partial_k} - \frac{\partial \bar{b}_j}{\partial_k}\frac{\partial \bar{u}_i}{\partial_k}\right). \tag{27}$$

A static model coefficient, $C = 1/12$, is used in this work, but this coefficient could be replaced by three coefficients computed using a dynamic procedure.[11,27]

4. Mixed gradient and Smagorinsky-like model (Mixed)

The gradient model was found to be unstable for LES of hydrodynamic turbulence and for LES of scalar-turbulent mixing.[6,28] Indeed, this model leads to an underestimation of the global GS/SGS transfers. Therefore, eddy diffusivity and viscosity can be added to the gradient model in order to increase the intensity of direct transfers. This mixed gradient and Smagorinsky-like (mixed) model was originally introduced in hydrodynamic[10] and was extended to incompressible MHD flows by Müller and Carati.[8] The models can be written using the following expressions:[15]

$$\tau_{ij}^{u} - \tau_{ij}^{b} = -C_\nu \Delta^2 |\bar{S}^u| \bar{S}_{ij}^u + \frac{\Delta^2}{12}\left(\frac{\partial \overline{u_i}}{\partial_k}\frac{\partial \overline{u_j}}{\partial_k}\right) - \frac{\Delta^2}{12}\left(\frac{\partial \overline{b_i}}{\partial_k}\frac{\partial \overline{b_j}}{\partial_k}\right), \tag{28}$$

$$\tau_{ij}^{ub} = -C_\lambda \Delta^2 |\vec{j}| \overline{J_{ij}} + \frac{\Delta^2}{12}\left(\frac{\partial \overline{b_i}}{\partial_k}\frac{\partial \overline{u_j}}{\partial_k} - \frac{\partial \overline{b_j}}{\partial_k}\frac{\partial \overline{u_i}}{\partial_k}\right), \tag{29}$$

where the coefficients are computed dynamically.[8]

B. Models performance in the non-helical case

1. A priori test

The SGS models are first evaluated through an *a priori* test performed on the non-helical case. Figure 9 shows the mean GS/SGS transfer predicted by each model for the kinetic (left) and magnetic (right) energy, as a function of the filter size. The mean exact GS/SGS transfers extracted from the filtered DNS are also shown for comparison. Note that the Grad model tends to underpredict the magnitude of the GS/SGS transfers as the filter size increases, for both kinetic and magnetic energies, which can lead to unstable simulations. This is a well-known behavior of this model when it is used for LES of hydrodynamic flows[9] or for LES of turbulent mixing.[28] Conversely, Smag and Mixed models overpredict the transfers. This should lead to stable simulations, but it could modify the energy balance. Finally, Cross model predicts a GS/SGS transfer of kinetic energy similar to Smag model, but it predicts no magnetic GS/SGS transfer. Note that Müller and Carati[8] have already shown this property, explaining that in LES performed with this SGS model, the lack of GS/SGS magnetic energy transfer is expected to be compensated by the transfer between GS kinetic and GS magnetic energies caused by the Lorentz force, term $T_{\bar{b}}^{\bar{u}}$. However, this will lead to a modification of the energy balance in LES computation, in comparison with DNS, and could lead to another flow dynamic.

Figure 10 shows PDF of GS/SGS transfers predicted by SGS models for kinetic (left) and magnetic (right) energies, for $\Delta/\Delta x = 8$. The PDF of exact transfers is also shown for comparison. As expected, for the kinetic energy GS/SGS transfer, Smag and Cross models appear as purely dissipative models, without prediction of backscatter. Mixed and Grad models predict backscatter, but the positive tails given by these models have rapid drops in comparison with the exact GS/SGS transfer, showing a strong underprediction of this phenomenon. All models also predict a more rapid drop of the negative tail in comparison with the exact GS/SGS transfer. This means that the models are not able to accurately predict the intermittent behavior of the forward scatter and the amplitude of the stronger events. Mixed model is the closest model to the filtered DNS, whereas the Cross model leads to the prediction of forward scatter event with the smallest amplitude. For the magnetic energy GS/SGS transfer, Smag model also appears as a dissipative model, as expected. Other models are able to predict backscatter, but with a strong underprediction in comparison with DNS. The Cross model predicts a very small amplitude of transfers

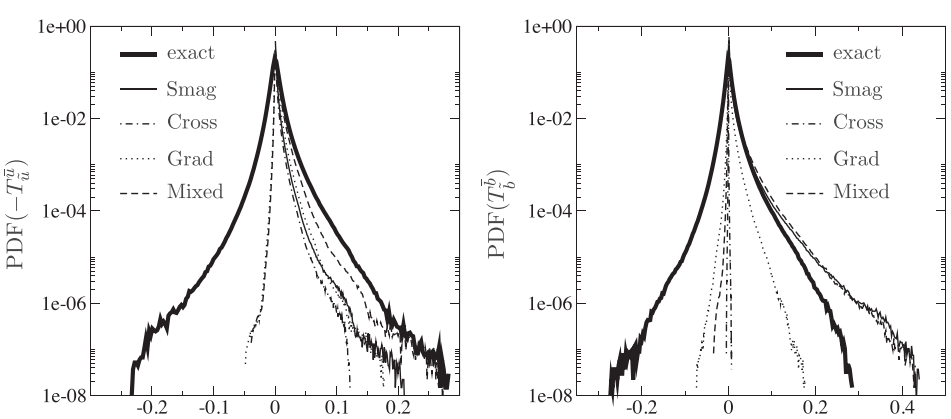

FIG. 10. Probability density function (PDF) of GS/SGS transfers for kinetic (left) and magnetic (right) energies at $\Delta/\Delta x = 8$, for the non-helical case. Comparison between SGS models and exact transfers.

(forward or backward), leading to globally no mean transfer. The Grad model predicts higher amplitude for both forward and backward transfers in comparison with the Cross model, but the model prediction remains notably weaker than the DNS results. Conversely, forward scatter is strongly over estimated by Smag and Mixed models with a negative tails higher than the DNS result, showing that models predict a more intermittent forward scatter phenomenon with a stronger amplitude. Note that similar behaviors have been found for other filter sizes (as long as the filter size is smaller than the forcing scale).

2. A posteriori test

To complete the analysis of SGS models performance, *a posteriori* tests are performed, and then, LES are performed for each set of SGS models on a mesh composed of 64^3 grid points. The initial condition is generated from DNS results at the saturated regime by using a spectral interpolation, which is equivalent to a spectral cut-off filtering. The LES results can thus be compared with filtered DNS results from the database.

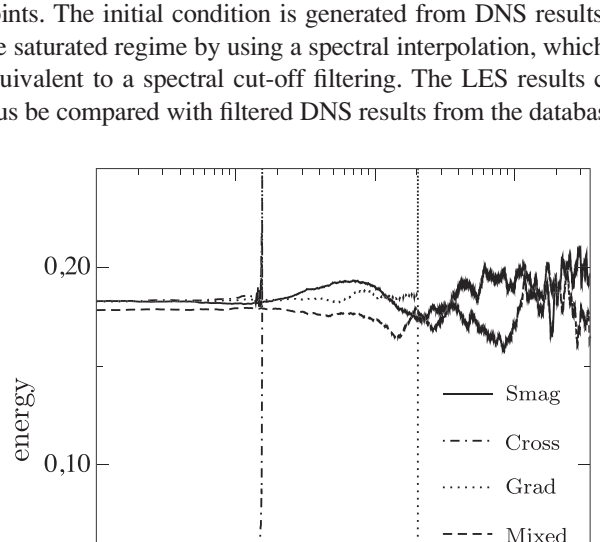

FIG. 11. Time evolution of resolved kinetic (higher value) and magnetic (lower value) energies in the non-helical case, for LES performed with Smag, Cross, Grad, and Mixed models.

Figure 11 shows the time evolution of the resolved kinetic and magnetic energies obtained from LES using various models. LES performed with Cross and Grad models lead to unstable simulations, with a significant growth of the resolved kinetic and magnetic energies. This behavior is well known with the Grad model for hydrodynamic[6] and MHD configurations.[8] This is due to local underpredictions of direct transfers, and to the production of backward transfers, for both kinetic and magnetic energies, as seen from *a priori* tests. These lead to an accumulation of energy at the smallest resolved scales as shown by Figure 12, which compares the kinetic and magnetic energy spectra of LES computations with DNS results. The energy accumulation characterizes the unstable behavior of the Grad model with the generation of non-physical fluctuations at these scales. The Cross model leads to an increase in the resolved magnetic energy from the beginning of the computation. This is because the Cross model does not provide any GS/SGS transfers for the magnetic energy, as seen with *a priori* tests. This leads to non-physical fluctuations of magnetic energy at the intermediate resolved scales (Fig. 12). Since the modeled GS/SGS transfer of the resolved kinetic energy depends on the magnetic strain rate tensor, a decay of the resolved kinetic energy is predicted initially, due to an overprediction of the direct GS/SGS transfer. However, non-physical fluctuations of the magnetic energy ultimately imply a disturbance of the resolved kinetic energy, and lead to an unstable simulation. Note that stable LES using the Cross model have been performed by Müller and Carati[8] in configurations without the dynamo effect. In this case, there is no source term of the magnetic energy, and the simulations are less sensitive to the absence of GS/SGS transfer for the magnetic energy. Conversely, Smag and Mixed models lead to stable simulations. The resolved kinetic and magnetic energies predicted by LES using these models are close to the value of the filtered DNS (which is the initial value, $t = 0$). Figure 12 compares the kinetic and magnetic energy spectra for both models, with the DNS results. The LES spectra are in good agreement with the DNS result. However, an underprediction of the magnetic energy spectra at the smallest resolved scales is observed. This probably corresponds to the over dissipation of the magnetic energy GS/SGS transfer observed in *a priori* tests for these models.

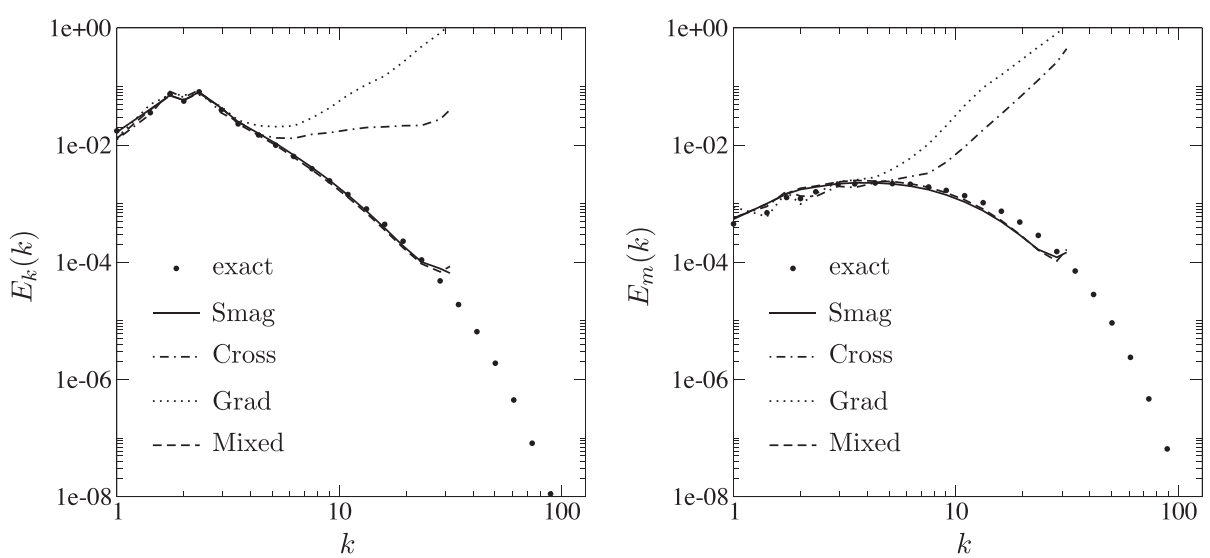

FIG. 12. Kinetic, $E_k(k)$ (left), and magnetic, $E_m(k)$ (right), energy spectra in the non-helical case. Comparison between DNS results and LES performed with Smag, Cross, Grad, and Mixed models. For stable simulations (DNS and LES using Smag and Mixed models), mean spectra are shown, whereas for unstable LES (using Cross and Grad models), instantaneous spectra are shown just before simulations divergence.

C. Models performance in the helical case

1. A priori test

The second flow configuration is now considered. This case is dominated mainly by magnetic energy, with inverse cascade at large scales and significant amount of helicity. It is therefore expected to be more demanding for SGS models. Because only Mixed and Smag models are stable in the non-helical case, only these both models are considered in this part.

These models are first evaluated through *a priori* tests. The global GS/SGS transfers for both kinetic and magnetic energies predicted by the models are evaluated for several filter sizes and are compared with filtered DNS results (referred as "exact" on figures), as shown in Figure 13. As for the non-helical case, a large over prediction of the magnitude of the transfers is found for both models, with the strongest over prediction still being found for the Mixed model.

PDF of GS/SGS transfers predicted by SGS models for the kinetic (left) and magnetic (right) energies are shown in Figure 14, with a comparison with filtered DNS results. As already shown, due to the domination of the magnetic energy, the exact kinetic energy GS/SGS transfer due to the Lorentz force and the exact magnetic energy GS/SGS transfer are more intermittent, and have stronger fluctuations than in the non-helical case. SGS models are not able to predict these behavior modifications, and the PDF of transfers predicted by Smag and Mixed models in the helical case is very similar to the PDF observed in the non-helical case. For the kinetic energy GS/SGS transfer, this implies that models are not able to predict the strongest forward scatter events, whereas the Mixed model result was close to the DNS result for the non-helical case. Since models overpredict the magnitude of the mean transfer, this means that the models predict forward scatter with less intermittency, and with a smaller level of fluctuations. The same trend is found for the direct magnetic energy GS/SGS transfers predicted by the Smag model, conversely to the non-helical case, where this model predicts a higher level of fluctuations in comparison with DNS data. The Mixed model appears in better

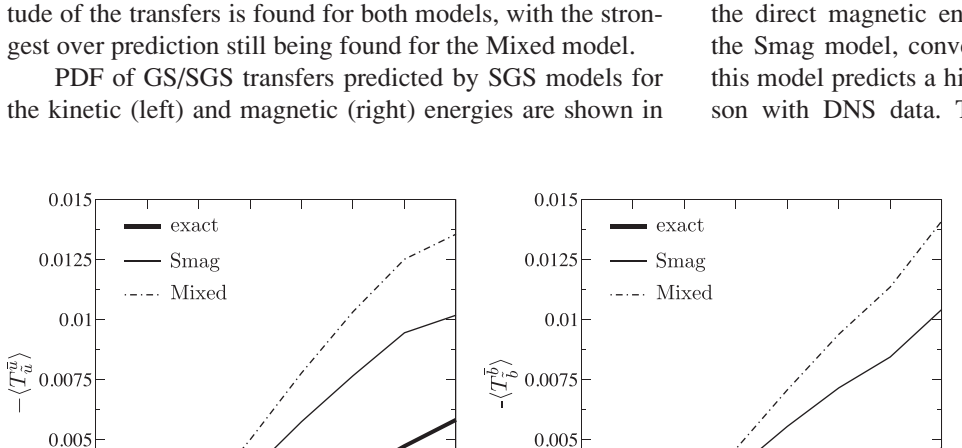

FIG. 13. Averaged GS/SGS transfers predicted by models as a function of the filter size, for both kinetic (left) and magnetic (right) energies, in the helical case. The exact transfers (from filtered DNS) are also shown for comparison.

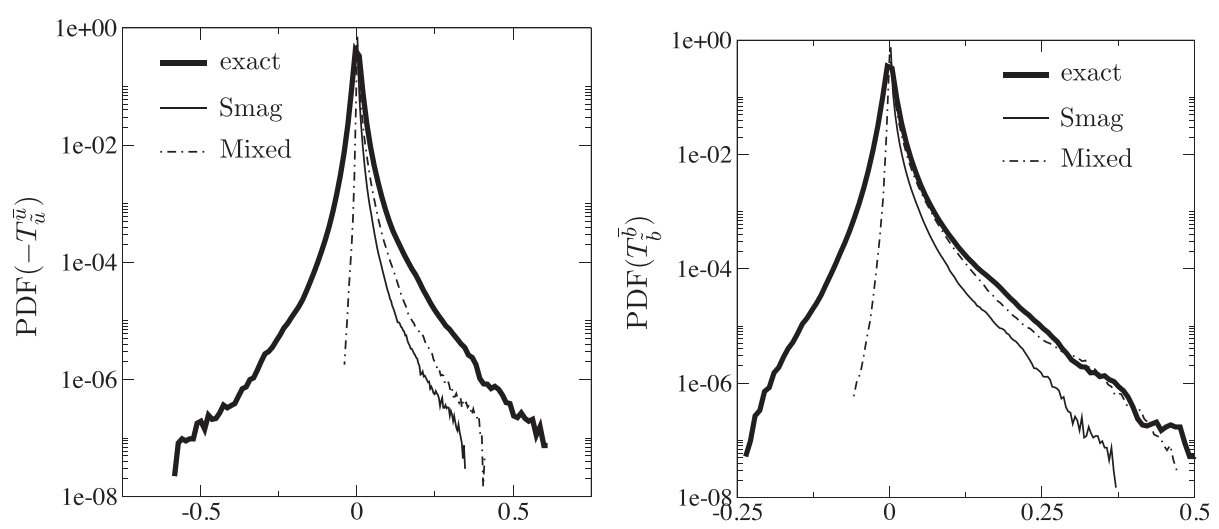

FIG. 14. Probability density function (PDF) of GS/SGS transfers for kinetic (left) and magnetic (right) energies at $\Delta/\Delta x = 8$, for the helical case. Comparison between SGS models and exact transfers (from filtered DNS).

agreement than the Smag model for the direct transfers, but it still underpredicts the backward scatter phenomenon.

2. A posteriori test

To complete the analysis of the SGS models' performance, *a posteriori* tests are now performed, similarly to the non-helical case. LES are still performed on a mesh composed by 64^3 grid points, starting from an initial condition extracted from the DNS results at the saturated regime.

In these tests, the behavior of both models is found to be similar; therefore, only the Smag model is discussed here. Figure 15 shows the time evolution of both resolved kinetic and magnetic energies for LES performed using the Smag model. This model (and Mixed model, not shown) leads to unstable simulation, with a rapid growth of both types of energy. As for the non-helical case, an accumulation of energy at the smallest resolved scales has been observed. To better understand this behavior, the power spectral density (PSD) of the GS/SGS kinetic and magnetic energy transfer is considered for both Smag model and DNS results. For a given quantity T in physical space, the PSD is defined as, $PSD(k) = \int_{|\vec{k}|=k} |\hat{T}|^2 d\vec{k}$, with $\hat{T}$ the Fourier transform of T, $\vec{k}$ a wave vector, and k the considered wave number. These quantities allow to reveal the scale repartition of the transfers. Figure 16 shows the PSD of the exact and modeled, kinetic, and magnetic energy GS/SGS transfers for helical and non-helical cases. The model leads to an over-prediction of transfer at larger scales and an under-prediction at smaller resolved scales, in comparison with DNS results for all the cases. Moreover, the DNS results show an intensification of both kinetic and magnetic transfers for the helical case in comparison with the non-helical case, at the smallest scales. The model used for the kinetic transfer is able to reproduce this. The model predicts then more intense transfer for the helical case. However, for the magnetic transfer, the PSD of the modeled term is less intense at these scales in the helical case than in the non-helical case. This leads to a stronger underdissipation at the smallest scales in the helical case, in comparison with the non-helical case. The energy is therefore accumulating at the smallest resolved scales, leading to an unstable simulation.

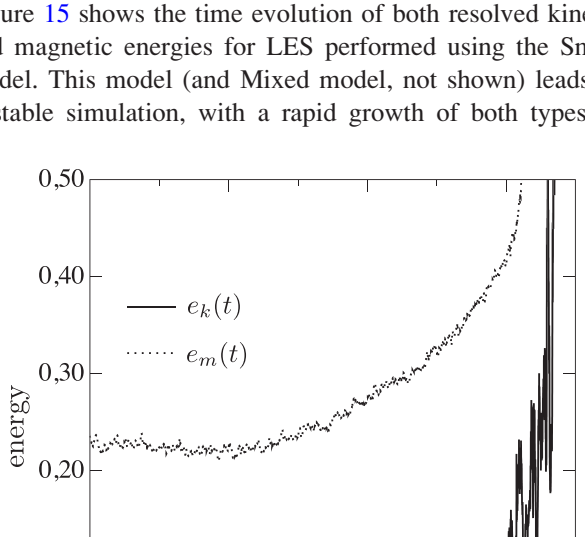

FIG. 15. Time evolution of resolved kinetic, $e_k(t)$, and magnetic, $e_m(t)$ energies in the helical case, for LES performed with the Smag model.

V. CONCLUSION

In this work, the grid-scale (GS) to subgrid-scale (SGS) energy transfers predicted by various SGS models are studied in the context of LES of MHD turbulent flows. The study is based on a database composed of DNS of two different flow configurations that differ mainly by the forcing scheme used to maintain the kinetic energy. In both cases, the magnetic energy is also maintained due to the dynamo effect, leading to statistically stationary saturated regimes. In the

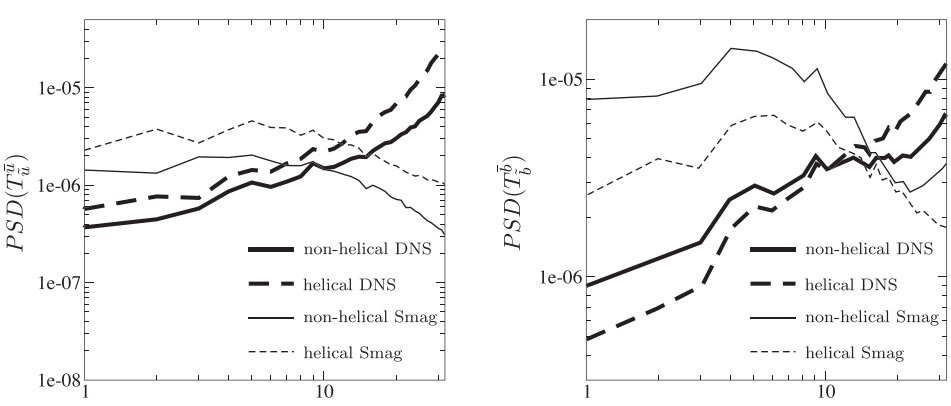

FIG. 16. Power spectral density (PSD) of the kinetic (left) and magnetic (right) energy GS/SGS transfers. Comparison between Smag model and DNS results for both helical and non-helical cases, for $\Delta/\Delta x = 8$.

second case, the forcing scheme allows the introduction of a large part of helicity in the flow leading to an inverse cascade of the magnetic energy at the largest scales.[1] The first case corresponds to a non-helical flow, where only a direct cascade of the magnetic energy occurs. Using scales separation, the exact equations of the GS/SGS kinetic and magnetic energies are derived. This allows the definition of the global energies balance of the flow and identification of the GS/SGS transfer terms for both kinetic and magnetic energies. From the DNS database, it is shown that the energy balance and the GS/SGS transfer terms are strongly dependent on the flow configurations. The capabilities to reproduce these GS/SGS transfers are then tested for various sets of SGS models. For the non-helical case, the gradient and the cross-helicity models are found to lead to unstable simulations, mainly because of an inappropriate reproduction of the magnetic energy GS/SGS transfer. For this flow configuration, the Smagorinsky-like and the mixed-gradient models allow stable LES, but with an overprediction of the GS/SGS transfers. For the helical case, which is mainly dominated by magnetic energy, these two models, the Smagorinsky-like and the mixed-gradient models, are not able to perform stable LES. This is mainly due to an important under prediction of the magnetic energy GS/SGS transfer at the smallest resolved scales. This analysis suggests that modeling effort has to be devoted mainly to improving the modeling of the SGS term of the induction equation, in order to improve the prediction of the GS/SGS transfers of magnetic energy. Finally, note that, in future work, other SGS models could be evaluated based on this analysis, as the scale-similarity model,[29] for example.

ACKNOWLEDGMENTS

The authors would like to thanks Nagi N. Mansour, Alexander Kosovichev, Irina Kitiashvili, and Alan Wray for fruitful discussion during M.K. and G.B. visit. The authors acknowledge support from region Rhône-Alpes through the CIBLE program and from the France-Stanford Center for Interdisciplinary Studies. This work was granted access to the high performance computing (HPC) resources of "Institut du développement et des ressources en informatique scientifique" (IDRIS) under the allocation 20142a0611 made by "Grand équipement national de calcul intensif" (GENCI), and to the Froggy platform of the "Calcul intensif, modélisation, expérimentation numérique et technologique" (CIMENT) infrastructure (https://ciment.ujf-grenoble.fr). ISTerre and LEGI are part of Labex OSUG@2020 (Grant No. ANR10LABX56) and Labex Tec21 (Grant No. ANR11LABX30).

[1]A. Brandenburg, "The inverse cascade and nonlinear alpha-effect in simulations of isotropic helical hydromagnetic turbulence," Astrophys. J. **550**(2), 824 (2001).
[2]N. E. Haugen, A. Brandenburg, and W. Dobler, "Simulations of nonhelical hydromagnetic turbulence," Phys. Rev. E **70**(1), 016308 (2004).
[3]M. L. Theobald, P. A. Fox, and S. Sofia, "A subgrid-scale resistivity for magnetohydrodynamics," Phys. Plasmas **1**, 3016 (1994).
[4]J. Smagorinsky, "General circulation experiments with the primitive equations," Mon. Weather Rev. **91**, 99 (1963).
[5]J.-P. Chollet and M. Lesieur, "Parameterization of small scales of three-dimensional isotropic turbulence utilizing spectral closures," J. Atmos. Sci. **38**, 2747 (1981).
[6]B. Vremen, B. Geurts, and H. Kuerten, "Large-eddy simulation of the turbulent mixing layer," J. Fluid Mech. **339**, 357–390 (1997).
[7]J. Baerenzung, H. Politano, Y. Ponty, and A. Pouquet, "Spectral modeling of magnetohydrodynamic turbulent flows," Phys. Rev. E **78**, 026310 (2008).
[8]W.-C. Muller and D. Carati, "Dynamic gradient-diffusion subgrid models for incompressible magnetohydrodynamic turbulence," Phys. Plasmas **9**(3), 824–834 (2002).
[9]A. Leonard, "Energy cascade in large-eddy simulations of turbulent fluid flows," in *Advances in Geophysics* (Elsevier, 1975), Vol. 18.
[10]R. A. Clark, J. H. Ferziger, and W. C. Reynolds, "Evaluation of subgrid-scale models using an accurately simulated turbulent flow," J. Fluid Mech. **91**(3), 1–16 (1979).
[11]H. Matsui and B. A. Buffett, "Sub-grid scale model for convection-driven dynamos in a rotating plane layer," Phys. Earth Planet. Inter. **153**(13),108–123 (2005).
[12]L. Jacoutot, A. G. Kosovichev, A. A. Wray, and N. N. Mansour, "Numerical simulation of excitation of solar oscillation modes for different turbulent models," APJ **682**, 1386–1391 (2008).
[13]J. Baerenzung, M. Holschneider, and V. Lesur, "Bayesian inversion for the filtered flow at the earth's core-mantle boundary," J. Geophys. Res.: Solid Earth **119**(4), 2695–2720, doi:10.1002/2013JB010358 (2014).
[14]O. Agullo, W.-C. Muller, B. Knaepen, and D. Carati, "Large eddy simulation of decaying magnetohydrodynamic turbulence with dynamic subgrid-modeling," Phys. Plasmas **8**(7), 3502–3505 (2001).
[15]G. Balarac, A. G. Kosovichev, O. Brugière, A. A. Wray, and N. N. Mansour, "Modeling of the subgrid-scale term of the filtered magnetic field transport equation," in Proceedings of the Summer Program on Center for Turbulence Research (2010).
[16]A. A. Chernyshov, K. V. Karelsky, and A. S. Petrosyan, "Subgrid-scale modeling for the study of compressible magnetohydrodynamic turbulence in space plasmas," Phys.-Usp. **57**(5), 421 (2014).

[17]B. A. Buffett, "A comparison of subgrid-scale models for large-eddy simulations of convection in the earth's core," Geophys. J. Int. **153**(3), 753–765 (2003).
[18]C. Canuto, M. Y. Hussaini, A. M. Quarteroni, and T. A. Zang, *Spectral Methods in Fluid Dynamics* (Springer, 1988).
[19]J.-B. Lagaert, G. Balarac, and G.-H. Cottet, "Hybrid spectral-particle method for the turbulent transport of a passive scalar," J. Comput. Phys. **260**, 127–142 (2014).
[20]R. Stepanov, F. Plunian, M. Kessar, and G. Balarac, "Systematic bias in the calculation of spectral density from a three-dimensional spatial grid," Phys. Rev. E **90**(5), 053309 (2014).
[21]M. Kessar, F. Plunian, R. Stepanov, and G. Balarac, "Non-kolmogorov cascade of helicity-driven turbulence," Phys. Rev. E **92**(3), 031004 (2015).
[22]K. Alvelius, "Random forcing of three-dimensional homogeneous turbulence," Phys. Fluids **11**(2), 1880 (1999).
[23]C. B. da Silva and O. Métais, "On the influence of coherent structures upon interscale interactions in turbulent plane jets," J. Fluid Mech. **473**(12), 103–145 (2002).
[24]A. Alexakis, P. D. Mininni, and A. Pouquet, "Shell-to-shell energy transfer in magnetohydrodynamics. I. Steady state turbulence," Phys. Rev. E **72**, 046301 (2005).
[25]M. Germano, U. Piomelli, P. Moin, and W. H. Cabot, "A dynamic subgrid-scale eddy viscosity model," Phys. Fluids **3**, 1760–1765 (1991).
[26]D. K. Lilly, "A proposed modification of the germano subgrid? Scale closure method," Phys. Fluids A: Fluid Dyn. (1989–1993) **4**(3), 633–635 (1992).
[27]H. Matsui and B. A. Buffett, "Characterization of subgrid-scale terms in a numerical geodynamo simulation," Phys. Earth Planet. Inter. **223**, 77–85 (2013).
[28]G. Balarac, J. Le Sommer, X. Meunier, and A. Vollant, "A dynamic regularized gradient model of the subgrid-scale scalar flux for large eddy simulations," Phys. Fluids (1994-present) **25**(7), 075107 (2013).
[29]A. Chernyshov, K. Karelsky, and A. Petrosyan, "Efficiency of scale-similarity model for study of forced compressible magnetohydrodynamic turbulence," Flow, Turbul. Combust. **89**(4), 563–587 (2012).